Supporting Information

Hwang and Varshavsky 10.1073/pnas.0808891105

SI Text

Some Missense Mutations at Position 277 of Ubr1 Can Affect Its in Vivo Half-Life. This part of our study is described largely in *SI Text*, because the metabolic-instability effect of Ubr1 alterations at position 277 described below could not be linked, thus far, to nonmutational modifications of Ubr1 at this position (see *Results*). To probe the functions of Ubr1 phosphorylation, each of its 8 phosphorylated residues (Fig. 1*B*) was mutated to Ala, a nonphosphorylatable small residue. The resulting Ubr1 derivatives were expressed in JD55 (*ubr1*Δ) *S. cerevisiae* from a low-copy plasmid and the native P_{UBR1} promoter and terminator. These cells also carried 1 of 2 high-copy plasmids that expressed, via the Ub fusion technique (1, 2), X-β-galactosidase (X-βgal) N-end rule substrates that contained, respectively, N-terminal Arg (a type-1 destabilizing residue) and N-terminal Tyr (a type-2 destabilizing residue) (Fig. 1*A*). Previous work has shown that the enzymatic activity of βgal in extracts from *S. cerevisiae* expressing X-βgal reporters was a reliable measure of these reporters' metabolic stability in vivo (1, 3). As expected, both Arg-βgal and Tyr-βgal were short-lived in vivo (low levels of βgal) in the presence of wild-type Ubr1 but were long-lived in the absence of Ubr1 (Fig. 2*B*). However, both Arg-βgal and Tyr-βgal became long-lived in cells containing $Ubr1^{Y277A}$ instead of wild-type Ubr1 (Fig. S2*B*). As described below, the functional inactivity of both $Ubr1^{Y277A}$ and $Ubr1^{Y277E}$ (where Glu^{277} is a "mimic" of phospho-Tyr) (Fig. S2 *B* and *C*) stemmed largely (possibly entirely) from their becoming short-lived *in vivo*, in comparison to either wild-type Ubr1 or $Ubr1^{Y277F}$, a different missense mutant at position 277 (Fig. S2 *D* and *E*).

Dipeptides bearing type-1 or -2 destabilizing N-terminal residues interact with the cognate (type-1 or -2) binding sites of Ubr1 and thereby activate, synergistically and allosterically, the third substrate-binding site of Ubr1. The third site mediates the targeting of Cup9, a transcriptional repressor of a regulon that includes the peptide transporter Ptr2 (see Introduction) (4–6). We assayed the import of dipeptides in [*ubr1*Δ *lys2*Δ] *S. cerevisiae*, a lysine (Lys)-requiring derivative of a *ubr1*Δ strain that carried plasmids expressing either $Ubr1^{Y277A}$ or other mutants of Ubr1 at position 277. [*ubr1*Δ *lys2*Δ] cells expressing either $Ubr1^{Y277A}$ or $Ubr1^{Y277E}$ were incapable of peptide import. Specifically, these cells did not grow on plates containing micromolar levels of Lys-Ala, a phenotype indistinguishable from that of [*ubr1*Δ *lys2*Δ] cells that lacked Ubr1 and therefore contained *PTR2*-repressing levels of Cup9 (Fig. S2*C*). In contrast, the same yeast strain that expressed either wild-type Ubr1 or $Ubr1^{Y277F}$ (containing Phe^{277}, a nonphosphorylatable aromatic-residue analog of wild-type Tyr^{277}) grew under these conditions, implying a viability-sustaining influx of the Lys-Ala dipeptide (Fig. S2*C*). Substantially higher (5 mM) levels of Lys-Ala in the medium could partially rescue the growth of cells expressing $Ubr1^{Y277A}$ but not of cells expressing $Ubr1^{Y277E}$ (Fig. S2*C*).

As a part of this study, we produced an affinity-purified rabbit polyclonal antibody to N-terminal half of *S. cerevisiae* Ubr1, denoted as $Ab1^{ScUBR1(1–1140)}$ (see *Results* and *SI Materials and Methods*). Unexpectedly, both $Ubr1^{Y277E}$ and $Ubr1^{Y277A}$ mutant proteins were virtually undetectable by immunoblotting extracts from the corresponding yeast strains with this antibody, in contrast to significant levels of (identically expressed) wild-type Ubr1 and some of its other mutants that could be detected (Fig. S2*D*). These results strongly suggested that $Ubr1^{Y277E}$ and $Ubr1^{Y277A}$ were short-lived in vivo. Pulse–chase analyses confirmed this conjecture, in that $Ubr1^{Y277E}$ was barely detectable even immediately after the pulse, in contrast to wild-type Ubr1 or $Ubr1^{Y277F}$ (Fig. S2*E*). Because Glu at position 277 in $Ubr1^{Y277E}$ was a negatively charged analog of the phospho-Tyr^{277} residue, these findings (Fig. S2 *D* and *E*) suggested, initially, that phosphorylation of wild-type Ubr1 on Tyr^{277} may also result in a short-lived Ubr1.

In vitro, Ubr1 appears to function as a monomer rather than, for example, a homodimer (7, 8). To determine whether the in vivo targeting of $Ubr1^{Y277E}$ for degradation was mediated, *in trans*, by other molecules of $Ubr1^{Y277E}$, or whether this short-lived Ubr1 mutant was targeted by another Ub ligase, we constructed and expressed $Ubr1^{Y277E,C1220S}$, a double-missense mutant. The previously characterized $Ubr1^{C1220S}$ is inactive as an E3, but its levels in vivo are not decreased relative to those of wild-type Ubr1 (3). In contrast to $Ubr1^{C1220S}$ but similarly to $Ubr1^{Y277E}$, the double-missense $Ubr1^{Y277E,C1220S}$ could not be detected upon expression in either wild-type or *ubr1*Δ strains (data not shown), indicating metabolic instability of this mutant, despite the inactivity of $Ubr1^{Y277E,C1220S}$ as an E3. We concluded that $Ubr1^{Y277E}$ was targeted for degradation by a non-Ubr1 Ub ligase. To identify the relevant E2 and/or E3, we examined degradation of $Ubr1^{Y277E}$ in *S. cerevisiae* strains that lacked specific E2 (Ub-conjugating) enzymes. A particularly strong stabilization of $Ubr1^{Y277E}$ was observed in *ubc13*Δ cells (Fig. S2 *F* and *G*). These cells lacked Ubc13, an E2 enzyme that functions in a complex that contains Mms2 and serves as an E2 partner of Rad5, a multifunctional protein with activities of both an E3 Ub ligase and DNA helicase. The Ubc13-Mms2-Rad5 complex interacts with another Ub ligase, Rad6-Rad18. The resulting machinery orchestrates either monoubiquitylation or Lys^{63}-based polyubiquitylation of PCNA, a sliding clamp on DNA and a major component of dynamic complexes that mediate DNA replication and repair (9–13).

$Ubr1^{Y277E}$, which is short-lived in wild-type *S. cerevisiae* (Fig. S2 *D* and *E*), was not stabilized in *rad5*Δ cells but was significantly stabilized in *mms2*Δ cells (as well as in *ubc13*Δ cells) and also, independently, in *rad18*Δ cells (Fig. S2 *F–H*). Taken together, these results indicated that $Ubr1^{Y277E}$ is targeted for degradation largely by Ub ligase complexes that involved the Ubc13-Mms2 E2 enzyme and the Rad18 E3. Yet another E2 ligand of Rad18 is Rad6 (10). The latter E2 is also an essential part of the Ubr1-Rad6 Ub ligase of the N-end rule pathway (14, 15). Rad18 may or may not interact with Ubc13-Mms2 directly and can be associated with it through the above-mentioned Rad5 Ub ligase in a multifunctional and incompletely understood circuit. Although our results (Fig. S2 *F–H*) indicate that the Ubc13-Mms2 E2 enzyme plays a role in degradation of $Ubr1^{Y277E}$, it should be noted that Ubc13-Mms2 has been known, thus far, to produce Lys^{63}-based polyUb chains, as distinguished from Lys^{48}-based chains that target a polyubiquitylated protein to the 26S proteasome (10). Lys^{63}-based polyUb chains target substrates for fates other than proteolysis. Nevertheless, recent evidence suggests that these chains can also target some proteins for degradation, either by the 26S proteasome or through autophagy (reviewed by ref. 16). In sum, we found, through the use of mutants, that $Ubr1^{Y277E}$ (and most likely $Ubr1^{Y277A}$ as well) is targeted for degradation by a Ub ligase that contains (at least) Ubc13, Mms2 and Rad18 (Fig. S2 *F–H*).

S. cerevisiae PCNA, a sliding DNA clamp, a replication/repair regulator, and a substrate of both Rad6-Rad18 and Ubc13-Mms2-Rad18, is targeted, at its Lys^{164} residue, either by these Ub

ligases, or by sumoylation enzymes (10, 17). The consensus sequence of sumoylation sites is ΨXKE, where Ψ can be Leu, Ile, Val, or Phe, and X is any residue (18–20). Lys^{209} and Lys^{276} of *S. cerevisiae* Ubr1 are parts of 2 putative sumoylation sites in the vicinity of (phosphorylated) Tyr^{277}. Mutational conversion of Lys^{276} to Arg, which cannot be sumoylated or ubiquitylated, did not significantly alter the in vivo levels of the resulting mutant Ubr1 protein, whereas the level of the $Ubr1^{K209R}$ mutant was significantly increased, in comparison to wild-type Ubr1 (Fig. S2*D*, lanes 6, 7; compare with lane 2). However, the double-missense $Ubr1^{K209R,Y277E}$, in which the K209R mutation was combined with the Ubr1-destabilizing Y277E mutation, remained a short-lived protein in vivo (data not shown), indicating that the bulk of metabolic instability of $Ubr1^{Y277E}$ did not involve reactions at Lys^{209}.

Metabolic Stability of $Ubr1^{pY277}$ (Ubr1 Phosphorylated on Tyr^{277}) Is Indistinguishable From That of Bulk Ubr1. We produced, affinity-purified and characterized 2 antibodies, $Ab1^{ScUbr1(1–1140)}$ and $Ab1^{pY277Ubr1}$, which recognized, respectively, all species of *S. cerevisiae* Ubr1 that retained its N-terminal half and specifically Ubr1 that had been phosphorylated on Tyr^{277} ($Ubr1^{pY277}$) (Fig. 2 *A–D*). Our findings with the $Ubr1^{Y277A}$ and $Ubr1^{Y277E}$ mutants (Fig. S2 *F–H*) indicated that the identity of a residue at position 277 is critical for a metabolically stable conformation of Ubr1. These findings preceded the production of the above antibodies and were, in fact, one reason for raising them. Surprisingly, however, the use of $Ab1^{ScUbr1(1–1140)}$ and $Ab1^{pY277Ubr1}$ (Fig. 2 *A–D*), and other approaches indicated that the metabolic stability of $Ubr1^{pY277}$ (wild-type Ubr1 phosphorylated on Tyr^{277}) was comparable to that of the bulk wild-type Ubr1, in contrast to short in vivo half-lives of $Ubr1^{Y277A}$ and $Ubr1^{Y277E}$ (Fig. S2 *D* and *E*). These reproducible, intriguing but (so far) functionally obscure results (Fig. S2 *B–E*) are therefore mentioned briefly and incompletely in the main text.

Materials and Methods

Yeast Strains, Media, Genetic Techniques, and β-Galactosidase Assay. The *S. cerevisiae* strains used in this study are described in Table S1. Standard techniques (21) were used for strain construction and transformation. The strains CHY50 (Δ*pdr5*::*KanMX6* Δ*ubr1*), CHY88 (Δ*mck1*::*KanMX6*), CHY89 (Δ*mck1*::*KanMX6* Δ*ubr1*), CHY201 (Δ*ubr1*::*KanMX6*), CHY202 (Δ*ubr1*::*KanMX6* Δ*yck1 yck2^{ts}*), CH203 (Δ*ubr1*::*SkHIS3MX6*), or CHY204 (Δ*ubr1*::*SkHIS3MX6* Δ*yck1 yck2^{ts}*) were constructed using one-step gene replacement and PCR-derived KanMX6 modules (22). E2 and E3 mutant strains used in this study were from the Varshavsky lab's yeast strain collection, or were purchased from Open Biosystems. The media for growing *S. cerevisiae* included YPD medium (1% yeast extract, 2% peptone, 2% glucose; only the most relevant media components are cited), SD medium (0.17% yeast nitrogen base, 0.5% ammonium sulfate, 2% glucose), SGal medium (0.17% yeast nitrogen base, 0.5% ammonium sulfate, 2% galactose), synthetic complete (SC) medium (0.17% yeast nitrogen base, 0.5% ammonium sulfate, 2% glucose, plus a dropout mixture of compounds required by a given auxotrophic strain), and SHM medium (0.17% yeast nitrogen base, 0.1% allantoin, 2% glucose). Assays for β-galactosidase (βgal) activity in *S. cerevisiae* extracts (1, 3, 23) were carried out by using the Yeast β-Galactosidase Assay Kit (Pierce), according to the manufacturer's protocol. The units of β-galactosidase activity were calculated as follows: unit = $1000 \times A_{420}/[(t) \times (v) \times (A_{660})]$, where ($t$) and ($v$) were the time of incubation (min) and the assay volume (ml), respectively.

Plasmids and Site-Directed Mutagenesis. The plasmids used in this study are described in Table S2. pRS315(-XbaI)UBR1 is a low copy (CEN-based) plasmid that expressed untagged wild-type Ubr1 from the native P_{UBR1} promoter (3). To produce counterparts of this plasmid that expressed mutant Ubr1 proteins, pRS315(-XbaI)UBR1 was digested with PstI/NotI, blunted and self-ligated, yielding pCH100, which contained only 1 SpeI site in the *UBR1* coding region. Overlapping extension PCR (24) was used to introduce specific mutations into the ORF of *UBR1*. A pair of PCR primers, OCH61 and OCH62 (Table S3), that flanked the region between the SpeI and *Pme*I sites of the *UBR1* ORF, was used. Multisite Ubr1 mutants ($Ubr1^{296A,S300A}$, $Ubr1^{S292A,S296A,S300A}$, $Ubr1^{T288A,S292A,S296A,S300A}$, and $Ubr1^{Y277F,T288A,S292A,S296A,S300A}$) were constructed sequentially by using specific plasmids as PCR templates: at first pCH121 (encoding $Ubr1^{S300A}$), then pCH122 (encoding $Ubr1^{S296A,S300A}$), then pCH123 (encoding $Ubr1^{S292A,S296A,S300A}$), and thereafter pCH224 (encoding $Ubr1^{T288A,S292A,S296A,S300A}$). Single-missense *UBR1* derivatives were constructed by using PCR primers described in Table S3, in conjunction with complementary-sequence primers. The resulting PCR products were digested with SpeI/*Pme*I and cloned into SpeI/*Pme*I-cut pCH100 or pFlagUBR1SBX (Table S2).

The high-copy pCH206 expressed, from the methionine-repressible P_{MET25} promoter, the Mck1 kinase C-terminally tagged with ha-RGSHis_6 (Qiagen) an ha-His_6-containing tag. To construct pCH206, the *MCK1* ORF was PCR-amplified from *S. cerevisiae* genomic DNA using OCH327 and OCH372 primers (Table S3). The resulting DNA fragment was cloned into BamHI/XhoI-cut pRS426MET25 vector (25), yielding pCH206. For site-directed mutagenesis of *MCK1*, mutations were introduced into the *MCK1* ORF using an approach similar to that used for mutagenesis of Ubr1. A pair of the above PCR primers for the cloning of pCH206 were used, in conjunctions with primers described below and the method of overlap extension PCR (24). For example, to construct pCH207 (Table S2), which expressed $Mck1^{D164A}$, 2 overlapping DNA fragments with a requisite missense mutation were produced at first, using PCR with the primer pairs OCH327/OCH353 and OCH329/OCH372 (Table S3). These fragments were then denatured and reannealed, so that that they formed a partially duplex DNA that encompassed the site of mutation and also contained 3′ overhangs that enabled another PCR, with the primers OCH327 and OCH372 (Table S3), that yielded the $MCK1^{D164A}$ ORF. DNA fragments produced by this procedure (they encoded either $Mck1^{D164A}$ or $Mck1^{Y99F}$) were digested with BamHI/XhoI and subcloned into BamHI/XhoI-cut pRS426MET25 vector, yielding, respectively, pCH207 and pCH212 (Table S2).

The high-copy pCH321 plasmid expressed Yck1-myc-His_7-CC (where the myc-His_7 epitopes were present immediately upstream of the C-terminal Cys-Cys palmitylation motif of Yck1) from the P_{ADH1} promoter. It was constructed as follows. The NcoI/XhoI-cut PCR product, produced using primers OCH531 and OCH532 (Table S3) and encoding the *YCK1* ORF with epitopes as described above was subcloned into NcoI/XhoI-cut pNTFlag717UBR1 (Table S2), replacing *UBR1* of the original plasmid with the *YCK1-myc-His-7-CC* ORF. pCH322 expressed the otherwise identical Yck1-myc-His_7-CC in which Lys^{98} was changed to Arg. pCH322 was constructed using overlapping PCR and the primer pairs OCH531/OCH534 and OCH533/OCH532 (Table S3).

Construction details for other plasmids (Table S2) are available upon request. All final plasmid constructs were verified by DNA sequencing.

Purification of Ubr1 and Mck1. The protease-deficient *S. cerevisiae* SC295 that carried pFlagUBR1SBX (Table S2) ("SBX" denotes the presence of SalI, BamHI and XhoI sites) and overexpressed the N-terminally flag-tagged Ubr1 (^{f}Ubr1) (5) was grown at 30° C to A_{600} of ≈4 in 4 l of SD medium containing Trp (20 μg/ml) and uracil (20 μg/ml). The cells were harvested by

centrifugation, washed once with cold PBS (PBS), and frozen in liquid N_2. Cells in a frozen pellet (20 g) were disrupted by grinding with a pestle in mortar containing 20 ml of lysis buffer (10% glycerol, 0.5% Nonidet P-40, 0.2 M KCl, 1 mM PMSF (Sigma-Aldrich) (added from a freshly prepared 0.1 M stock solution in ethanol), 10 mM NaF, 0.5 mM $NaVO_3$, 10 mM β-glycerol phosphate, 50 mM Hepes, pH 7.5) containing protease inhibitor mixture "for use with fungal and yeast extracts" (Sigma-Aldrich). The suspension was centrifuged at 11,200 $\times$ *g* for 30 min, and the supernatant was mixed with 2 ml of anti-flag M2 affinity beads (Sigma-Aldrich) at 4° C for 1 h. The beads were collected by centrifugation in Sorvall RT-600B at 1,000 rpm for 5 min at 4°C and were washed, sequentially, with 10 ml of lysis buffer, 10 ml of buffer A (10% glycerol, 0.5% Nonidet P-40, 1 M KCl, 1 mM EDTA, 10 mF NaF, 0.5 mM $NaVO_3$, 10 mM β-glycerol phosphate, 50 mM Hepes, pH 7.5), and 10 ml of buffer B (lysis buffer without Nonidet P-40). The anti-flag antibody-bound ^{f}Ubr1 was eluted with buffer C (buffer B containing flag peptide at 0.5 mg/ml) and thereafter dialyzed at 4° C overnight against 50 mM $(NH_4)_2CO_3$, pH 8.0. For Mck1-based kinase and ubiquitylation assays, ^{f}Ubr1 and ^{f}Ubr1^{Y277F} were purified as above from the SC295, CHY89 or BY1137 strains (Table S1) that carried either pFlagUBR1SBX or pCH119 (Table S2).

S. cerevisiae Mck1 C-terminally tagged with ha-RGSHis$_6$ was purified from SC295 cells that overexpressed the tagged Mck1 from pCH206 (Table S2). Expression of Mck1-ha-RGSHis$_6$ was induced by growing cells for 24 h at 30° C in 2 L of SD medium containing Leu (20 μg/mL) and His (20 μg/mL). Cells were collected by centrifugation, washed in cold PBS, rapidly frozen in liquid N_2, and subsequently lysed in buffer *D* (145 mM NaCl, 0.1% Tween 20, 5 mM imidazole, 50 mM Na-phosphate, pH 7.5) containing protease inhibitors (10 μg/mL aprotinin, 10 μg/mL leupeptin, 1 mM benzamidine, 2 μg/mL pepstatin, 0.5 mM PMSF). The lysate was passed through 2 mL of Ni-NTA beads (50% slurry) (Qiagen) previously equilibrated in buffer D. The beads were washed with 10 ml of buffer D and washed again with 6 ml of buffer D containing 20 mM imidazole. Mck1-ha-RGSHis$_6$ (or its mutant derivatives) was then eluted with 3 mL of buffer D containing 0.2 M imidazole. These fractions were pooled and dialyzed overnight against 2 L of buffer E (25% glycerol, 1 mM EDTA, 50 mM Mes, pH 6.5). Further purification involved chromatography of the dialyzed sample on a 5-mL column of Mono-S Sepharose (GE Healthcare) equilibrated with buffer E. The column was washed with 20 mL of buffer E, and Mck1-ha-RGSHis$_6$ (or its mutant derivatives) was eluted with 20 mL of buffer E and a linear gradient of NaCl up to 1 M, using FPLC. The eluted fractions were analyzed by SDS-NuPAGE (4–12%) (Invitrogen), followed by Coomassie staining or immunoblotting with anti-HA antibody (Sigma-Aldrich).

Determination of Phosphorylation Sites in Ubr1. Purified *S. cerevisiae* ^{f}Ubr1 (250 pmoles (51 μg) was reduced with 2 mM DTT in 50 mM $(NH_4)_2CO_3$ (pH 8.0) at 56° C for 1 h, and thereafter alkylated with 20 mM iodoacetamide in the presence of 6 M urea (in the dark) for 45 min at room temperature. The sample (50 μL) suspension was then digested with 50 μL of immobilized TPCK trypsin (Pierce) overnight at 37° C. Phosphopeptides in the resulting sample were either enriched first, using the phosphopeptide isolation kit (Pierce) or were directly analyzed by nanoscale-microcapillary reversed phase liquid chromatography and tandem mass spectrometry (cLC-MS/MS), using the QSTAR XL quadrupole time of flight mass spectrometer (Applied Biosystems). Phosphorylation sites were assigned by manual inspection of MS/MS spectra and also using the Mascot search engine (Matrix Science). The entire cycle of these MS-based procedures was carried out several times, until subsequent analyses did not yield additional phosphorylation sites.

Antibody to *S. cerevisiae* Ubr1. Ubr1$^{1–1140f}$, the C-terminally flag-tagged N-terminal half of the 1,950-residue wild-type *S. cerevisiae* Ubr1, was produced and purified as described (5, 15) and was used to produce rabbit antisera (Covance). After standard cycles of boost injections of the antigen, 10 mL of antiserum (after the third boost) were incubated overnight at 4° C (with gentle rocking) with 1 mL of CNBr-Sepharose (GE Healthcare) that had been conjugated to purified full-length (flag-tagged) ^{f}Ubr1 (≈1 mg). The incubated suspension was loaded into a 5-mL plastic column (Pierce), letting excess liquid flow from Sepharose beads. The column was washed with 20 mL of PBS. Antibodies bound to ^{f}Ubr1-Sepharose were eluted (in 0.5-mL increments) with 5 mL of 0.1 M glycine (pH 2.5); the pH of eluted factions was adjusted to 8.0 with 1 M Tris immediately after elution. The first 6 of 0.5-mL fractions were pooled and incubated overnight at 4° C (with gentle rocking) with 1 mL of CNBr-Sepharose that had been conjugated to proteins of crude extract from Ubr1-lacking JD55 (*ubr1*Δ) cells, followed by the loading onto a plastic column, as described above. The flowthrough from that column, which contained a doubly affinity-purified (both "positively" and "negatively") anti-Ubr1 antibody, was incubated for 2 h at 4° C with 0.25 mL of gamma-bind Sepharose (GE Healthcare) that contained covalently bound Protein G. The bound antibodies were eluted with 0.1 M glycine (pH 2.5) and immediately adjusted to pH 8.0, as described above. Pooled fraction of eluted anti-Ubr1 were dialyzed at 4° C overnight against PBS buffer, followed by the addition of glycerol to the final concentration of 10%. After measuring the concentration of protein in thus purified anti-Ubr1 antibody sample (by measuring A_{280}), the antibody (0.15 μg/μL), which was termed Ab1$^{ScUbr1(1–1140)}$, was stored in multiple smaller samples at -80° C. For immunoblotting with Ab1$^{ScUbr1(1–1140)}$, preblocked Immobilon-P PVDF membrane (Millipore) was incubated with the affinity-purified Ab1$^{ScUbr1(1–1140)}$ (1:2,000) in a blocking buffer (5% nonfat milk, 0.5% Tween 20 in PBS) for 2 h, followed by standard postincubation immunoblotting procedures, with signal detection using SuperSignal Western Blotting kit (Pierce).

Antibody That Recognized Ubr1^{pY277}, Phosphorylated at Position 277. The phosphopeptide *C*QFLNDLKpY^{277}ENDY, from the sequence of *S. cerevisiae* Ubr1 shown in Fig. S2*A* and with the additional N-terminal Cys residue for conjugation to the carrier protein keyhole limpet hemocyanin, was synthesized by Abgent, which also synthesized a nonphosphorylated counterpart of this peptide and produced rabbit antisera to *C*QFLNDLKpY^{277}ENDY. Antibodies that bound to *C*QFLNDLKpY^{277}ENDY, were "positively" selected from immune sera by affinity chromatography on a resin derivatized with the above phosphopeptide immunogen. The resulting samples were then "negatively" selected by passing them through a resin derivatized with the unphosphorylated version of the same peptide. To further increase the specificity of this antibody sample for Ubr1 phosphorylated at Tyr^{277}, yet another step of "negative" selection was used. 2 mL of the above-purified antibody (≈1 mg of protein) was incubated overnight at 4° C (with gentle rocking) with 0.25 mL of glutathione-Sepharose (GE Healthcare) that had been conjugated to a mixture of 125 μg of GST-Ubr1$^{227–327}$ and 125 μg of GST-Ubr1$^{227–327,Y277F}$. These fusions of GST to the Ubr1$^{227–327}$ fragment (and its Y277F mutant counterpart) were produced in *Escherichia coli* BL21-CodonPlus (DE3)-RIL (Stratagene) carrying either pCH126 or pCH127 (Table S2) and were purified using glutathione-Sepharose gel according to the manufacturer's protocol. The resulting antibody, denoted as Ab1^{pY277Ubr1}, was used to detect Tyr^{277} phosphorylation of Ubr1 in yeast extracts by immunoblotting. The incubations were for 4 h at room temperature at the 1:1,000 dilution in 5% skin milk in PBST (PBS containing 0.5%

Tween 20). The bound antibody was detected with a goat anti-rabbit antibody (at 1:2,000 dilution) conjugated to horseradish peroxidase (HRP; Bio-Rad). The above (affinity-purified) Ab1^{Y277Ubr1} antibody was produced by 1 of 2 rabbits immunized with *C*QFLNDLKpY^{277}ENDY. The other immunized rabbit produced antibody that recognized both Ubr1^{pY277F} and unphosphorylated Ubr1. It was termed Ab2$^{p/non\text{-}pY277Ubr1}$ and was used for detection of bulk Ubr1.

Preparation of Cell Extracts for Immunoblotting. In part to optimize the preparation of yeast extracts for screening, by immunoblotting, for a kinase mutant that may be defective in phosphorylating Ubr1 at Tyr^{277}, we slightly modified an earlier method (26). *S. cerevisiae* (Table S1) were grown to A_{600} of ≈1 in SD with additional ingredients for a strain's auxotrophic requirements, and the amount of cells corresponding to 1 mL at A_{600} of 1 was pelleted by centrifugation at 11,200 × *g* for 1 min. Cells were resuspended and incubated in 1 mL of 0.2 M NaOH for 20 min on ice or (alternatively) for 5 min at room temperature, followed by centrifugation for 30 sec at 11,200 × *g*. The pelleted cells were resuspended in 50 μL of HU buffer (8 M urea, 5% SDS, 1 mM EDTA, 0.1 M DTT, 0.005% bromophenol blue, 0.2 M Tris·HCl, pH 6.8) containing 1× protease inhibitor mixture "for use with fungal and yeast extracts" (Sigma-Aldrich) and heated for 10 min at 70° C. After centrifugation for 5 min at 11,200 × *g*, 10 μL of supernatant was subjected to SDS/PAGE (4–12% NuPAGE; Invitrogen), followed by immunoblotting with anti-flag, anti-ha, and antitubulin antibodies (Sigma), and also with affinity-purified antibodies to either N-terminal half of the 225-kDa *S. cerevisiae* Ubr1 or to a synthetic phospho-Tyr-containing phosphopeptide of Ubr1 that encompassed position 277 (Fig. S2*A* and below). For yeast mutants in kinases of the Gsk3 family and other yeast strains used in kinase screens, see Table S1. Immunoblotting with anti-tubulin antibody was used as a protein-loading control, after stripping previous signal with Restore plus Western blot stripping buffer (Pierce).

Pulse–Chase Assays. *S. cerevisiae* JD55 (*ubr1*Δ) carrying plasmids expressing wild-type Ubr1 (pCH100), Ubr1^{Y277A} (pCH109), Ubr1^{Y277E} (pCH117), or Ubr1^{Y277F} (pCH118) were grown at 30° C to A_{600} of ≈1 in 10 ml of SC(-Leu) medium. Cells were pelleted by centrifugation and washed with 0.8 ml of SC medium lacking Leu and Met. Cell pellets were gently resuspended in 0.4 ml of the same medium and labeled for 5 min at 30° C with 0.16 mCi of ^{35}S-EXPRESS (Perkin-Elmer). Cells were pelleted again and resuspended in 0.4 ml of SC(-Leu) containing cold 10 mM methionine and 5 mM cysteine. Samples (0.1 ml) were taken at the indicated time points, followed by preparation of extracts, immunoprecipitation with affinity-purified anti-UBR1 antibody(1 μg), SDS-NuPAGE (4–12%), and autoradiography.

In Vitro Kinase Assays. Our early attempts to identify a kinase responsible for Ubr1 phosphorylation on Tyr^{277} included a "biochemical" screen that used biotin-ERAQFLNDLK*Y*^{277} ENDYMFDG, a biotinylated Ubr1-derived peptide substrate, and glutathione transferase (GST) fusions to specific yeast kinases (27, 28). This approach yielded Ptk2 and Tpk1. However, these kinases also phosphorylated both GST-Ubr1$^{227–327}$ and GST-Ubr1$^{227–327,Y277F}$, which were purified after their expression in *E. coli* (data not shown), making it unlikely that Ptk2 or Tpk1 were the cognate kinase(s) we sought. In a different and eventually successful approach, we used immunoblotting with the Ab1^{pY277Ubr1} antibody and a library of yeast mutants in 27 putative Try kinases, as described in the main text. The procedures described below were used after that screen (Fig. 2 *J* and *K*), which identified Mck1 as a cognate Ubr1 kinase.

Purified wild-type ^{f}Ubr1 unphosphorylated at Tyr^{277} (purified from *mck1*Δ cells; see *Results*) or ^{f}Ubr1^{Y277F} (which cannot be phosphorylated at position 277) were incubated (0.1 μg of Ubr1 and 0.1 μg of either wild-type Mck1 or enzymatically inactive Mck1^{D164A}) in 20 μl of kinase buffer (20 μM ATP, 10 mM $MgCl_2$,50 mM Tris·HCl, pH 7.5) containing 2 μCi of [γ-^{32}P]ATP (6,000 Ci/mmol). The reaction was stopped by adding 6 μl of 4× SDS loading buffer, followed heating for 5 min at 95° C, SDS/PAGE (4–12% NuPAGE; Invitrogen), the drying of a gel and autoradiography, either with PhosphorImager (Molecular Dynamics), or with x-ray films and intensifying screen at −80° C.

Pull-down assays and in vitro kinase assays with myc-tagged Yck1 were carried out as follows. A yeast extract (2 mg), produced using a modification of the earlier procedure (26) (see above) was precipitated with anti-myc antibody (Sigma) and protein G-magnetic beads (Invitrogen) in lysis buffer (0.2 M KCl, 1 mM EDTA, 10 mM β-mercaptoethanol, 1 mM PMSF, 50 mM Hepes, pH 7.5) containing inhibitor mixture "for use with fungal and yeast extracts" (Sigma-Aldrich). The beads were washed thrice in 0.5 mL of lysis buffer that also contained 0.3 M NaCl, and twice in kinase reaction buffer (40 μM ATP, 0.1 M NaCl, 10 mM $MgCl_2$, 0.2 mM DTT, 50 mM Tris·HCl, pH 7.5) containing the above protease inhibitor mixture. The resulting immunoprecipitate was resuspended in 25 μL of kinase buffer containing 4μCi of [γ-^{32}P]ATP and 2.5 μg of ^{f}Ubr1 or GST-Ubr1$^{227–327}$ as substrates. The two substrates were purified, respectively, from SC295 *S. cerevisiae* and BL21-CodonPlus (DE3)-RIL *E. coli*. The reaction was performed at 30° C for 30 min and stopped by the addition of 10 μl of 4×SDS/PAGE loading buffer, followed by heating 95° C for 5 min; 15 μL of each sample were subjected to SDS-10% PAGE, followed by Coomassie staining and autoradiography.

1. Suzuki T, Varshavsky A (1999) Degradation signals in the lysine-asparagine sequence space. *EMBO J* 18:6017–6026.
2. Varshavsky A (2005) Ubiquitin fusion technique and related methods. *Methods Enzymol* 399:777–799.
3. Xie Y, Varshavsky A (1999) The E2–E3 interaction in the N-end rule pathway: the RING-H2 finger of E3 is required for the synthesis of multiubiquitin chain. *EMBO J* 18:6832–6844.
4. Turner GC, Du F, Varshavsky A (2000) Peptides accelerate their uptake by activating a ubiquitin-dependent proteolytic pathway. *Nature* 405:579–583.
5. Du F, Navarro-Garcia F, Xia Z, Tasaki T, Varshavsky A (2002) Pairs of dipeptides synergistically activate the binding of substrate by ubiquitin ligase through dissociation of its autoinhibitory domain. *Proc Natl Acad Sci USA* 99:14110–14115.
6. Homann OR, Cai H, Becker JM, Lindquist SL (2005) Harnessing natural diversity to probe metabolic pathways. *PLoS Genet* 1:e80.
7. Bartel B, Wünning I, Varshavsky A (1990) The recognition component of the N-end rule pathway. *EMBO J* 9:3179–3189.
8. Du F (2001) PhD thesis (California Institute of Technology, Pasadena, CA).
9. Hoege C, Pfander B, Moldovan GL, Pyrowolakis G, Jentsch S (2002) RAD6-dependent DNA repair is linked to modification of PCNA by ubiquitin and SUMO. *Nature* 419:135–141.
10. Ullrich HD (2005) The RAD6 pathway: control of DNA damage bypass and mutagenesis by ubiquitin and SUMO. *ChemBioChem* 6:1735–1743.
11. Tomida J, *et al.* (2008) DNA damage-induced ubiquitylation of RFC2 subunit of replication factor C complex. *J Biol Chem* 283:9071–9079.
12. Loring GL, Christensen KC, Gerber SA, Brenner C (2008) Yeast Chfr homologs retard cell cycle at G1 and G2/M via Ubc4 and Ubc13/Mms2-dependent ubiquitination. *Cell Cycle* 7:96–105.
13. Fu Y, *et al.* (2008) Rad16-Rad18 mediates a eukaryotic SOS response by ubiquitinating the 9–1-1 checkpoint clamp. *Cell* 133:601–611.
14. Dohmen RJ, Madura K, Bartel B, Varshavsky A (1991) The N-end rule is mediated by the UBC2 (RAD6) ubiquitin-conjugating enzyme. *Proc Natl Acad Sci USA* 88:7351–7355.
15. Xia Z, *et al.* (2008) Substrate-binding sites of UBR1, the ubiquitin ligase of the N-end rule pathway. *J Biol Chem* 283:24011–24028.
16. Li W, Ye Y (2008) Polyubiquitin chains: Functions, structures and mechanisms. *Cell Mol Life Sci* 65:2397–2406.
17. Moldovan GL, Pfander B, Jentsch S (2007) PCNA, the maestro of the replication fork. *Cell* 129:65–79.
18. Wilson VG, Heaton PR (2008) Ubiquitin proteolytic system: focus on SUMO. *Expert Rev Proteom* 5:121–135.
19. Anckar J, Sistonen L (2007) SUMO: Getting it on. *Biochem Soc Trans* 35:1409–1413.
20. Geiss-Friedlander R, Melchior F (2007) Concepts in sumoylation: A decade on. *Nat Rev Mol Cell Biol* 8:947–956.

21. Ausubel FM, *et al*. (2006) *Current Protocols in Molecular Biology* (Wiley-Interscience, New York).
22. Longtine MS, *et al*. (1998) Additional modules for versatile and economical PCR-based gene deletion and modification in *Saccharomyces cerevisiae*. *Yeast* 14:953–961.
23. Baker RT, Varshavsky A (1991) Inhibition of the N-end rule pathway in living cells. *Proc Natl Acad Sci USA* 87:2374–2378.
24. Ho SN, Hunt HD, Horton RM, Pullen JK, Pease LR (1989) Site-directed mutagenesis by overlap extension using the polymerase chain reaction. *Gene* 77:51–59.
25. Mumberg D, Muller R, Funk M (1994) Regulatable promoters of Saccharomyces cerevisiae - comparison of transcriptional activity and their use for heterologous expression. *Nucleic Acids Res* 22:5767–5768.
26. Kushnirov VV (2000) Rapid and reliable protein extraction from yeast. *Yeast* 16:857–860.
27. Zhu H, *et al*. (2000) Analysis of yeast protein kinases using protein chips. *Nat Genet* 26:283–289.
28. Moriya H, Johnston M (2004) Glucose sensing and signaling in Saccharomyces cerevisiae through the Rgt2 glucose sensor and casein kinase I. *Proc Natl Acad Sci USA* 101:1572–1577.

A

Identified peptide	Phosphorylation site
pYENDYMFDGTTTAK	Y277
YENDYMFDGT**pT**TAK	T288
pT*pS*PSNSPEASPSLAK	S292 (T291)
pT*pS*PSN**pS**PEASPSLAK	S292 (T291), S296
pT*pS*PSNpSPEA**pS**PSLAK	S292 (T291), S296, S300
EHE**pS**EFDEQDNDVDMVGEK	S1196
NLDEDD**pS**DDNDDSDER	S1938
NLDEDD**pS**DDNDD**pS**DER	S1938, S1944

B

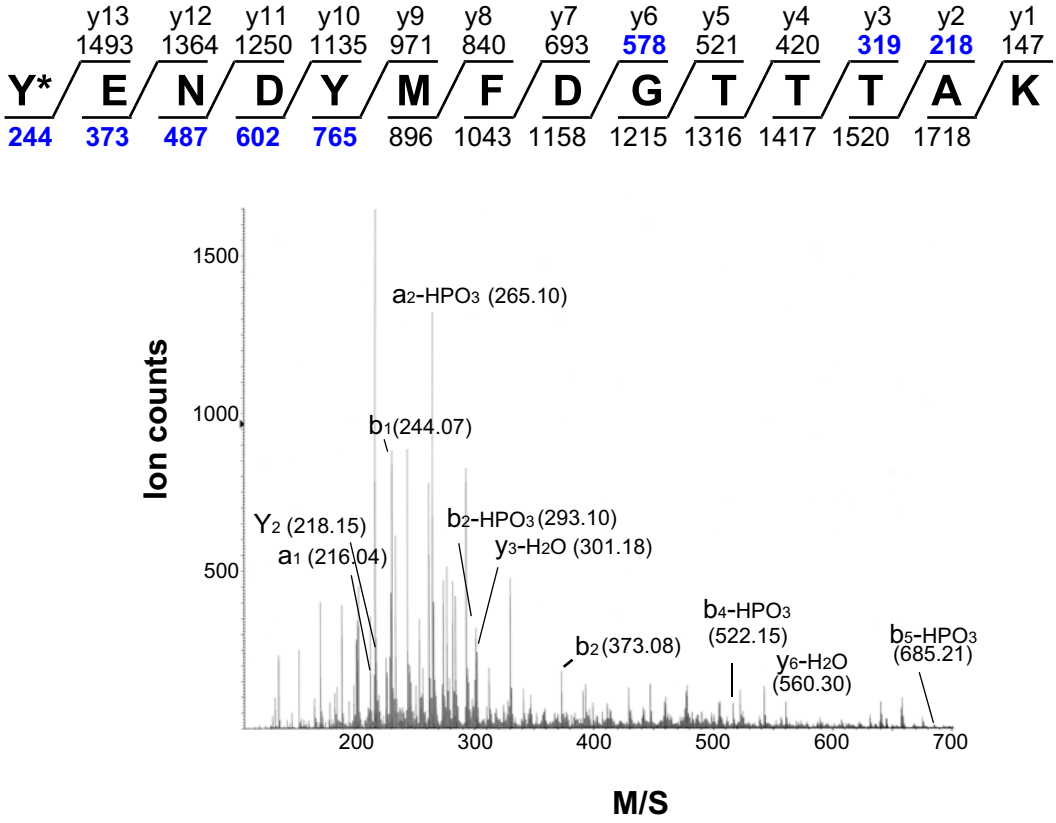

Fig. S1. Identification of *S. cerevisiae* Ubr1 phosphopeptides and phosphorylation sites using cLC-MS/MS. See *SI Materials and Methods*. (*A*) Identified phosphopeptides of Ubr1. Phosphorylated residues are in red, preceded by the prefix ''p.'' As indicated in the diagram, this approach could not distinguish between phosphorylation at Ser^{292} vs. Thr^{291}. Because the subsequently produced $Ser^{292} \rightarrow Ala^{292}$ (S292A) mutation in Ubr1 abolished phosphorylation at Tyr^{277} (see the main text and Fig. 1*C*), it is very likely that the in vivo phosphorylation of Ubr1 involves Ser^{292}. (*B*) Mass spectrometric analysis of a phosphopeptide containing phospho-Tyr^{277} (pY277), shown as an example of cLC-MS/MS experiments. The observed molecular masses of some peaks are indicated.

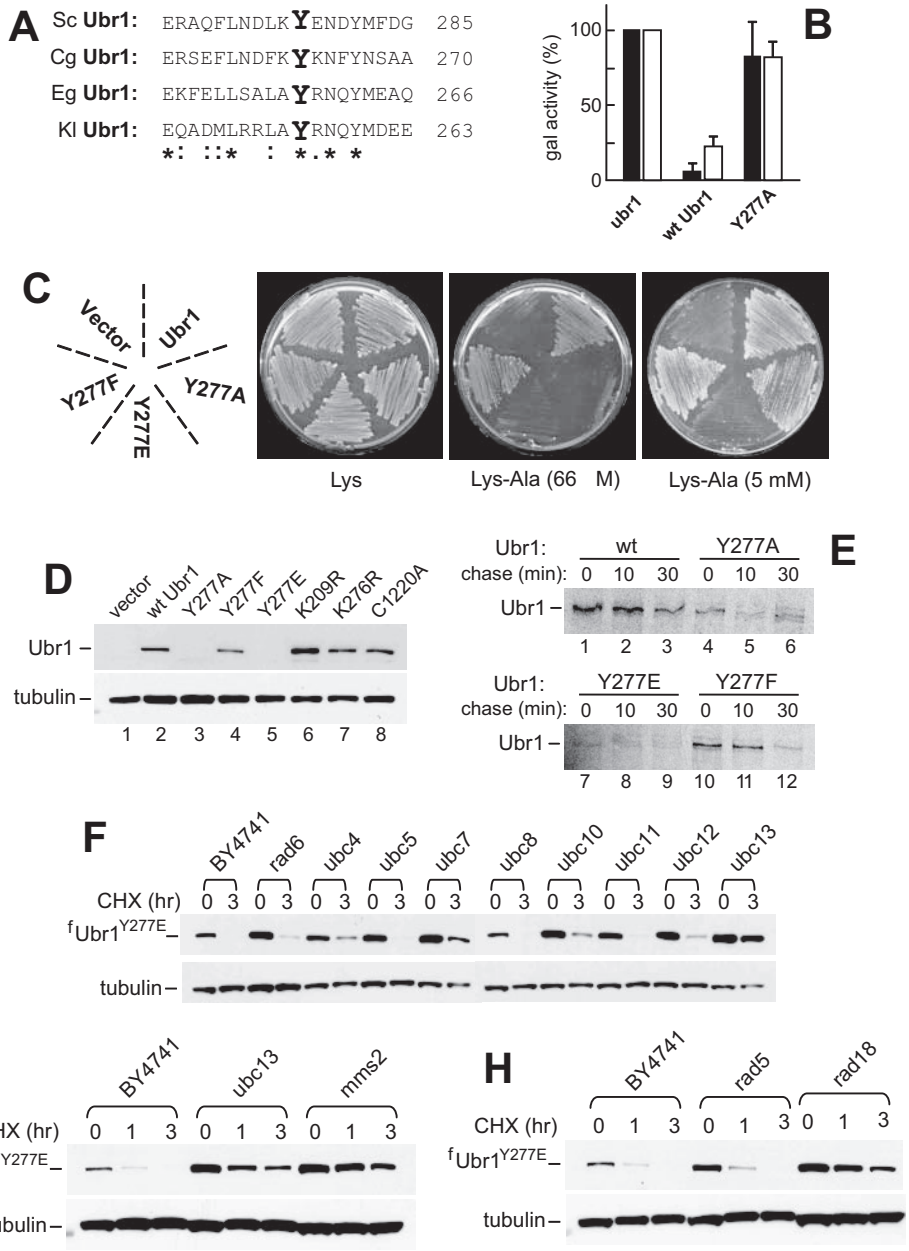

Fig. S2. Conversion of Tyr^{277} of *S. cerevisiae* Ubr1 to Ala or Glu makes the resulting Ubr1 proteins short-lived in vivo. (*A*) Conservation of Tyr^{277} and its environs in Ubr1 proteins of fungi: *S. cerevisiae* (Sc), *Candida glabrata* (*Cg*), *Eremothecium gossypii* (*Eg*), and *Kluyveromyces lactis* (*Kl*). Asterisks, colons and a dot denote identical, similar, and partially conserved residues, respectively. (*B*) Relative levels (enzymatic activity) of Arg-βgal (filled bars) and Tyr-βgal (white bars), a type-1 and a -2 N-end rule substrate, respectively (Fig. 1*A*), in *ubr1*Δ *S. cerevisiae* or in the same strain that expressed either wild-type Ubr1 or Ubr1^{Y277A}. (*C*) Relative efficiencies of dipeptide import in cells containing mutations in Ubr1 at position 277. JD55 (*ubr1*Δ) cells expressing either a vector control (pRS315), or wild-type Ubr1 (pCH100), or Ubr1^{Y277A} (pCH109), or Ubr1^{Y277E} (pCH117), or Ubr1^{Y277F} (pCH118) were streaked on plates containing 110 μM Lys (20 μg/mL) or Lys-Ala, at either 66 μM or 5 mM, followed by incubation at 30° C for 3 days. (*D*) Relative levels of wild-type and mutant Ubr1 proteins in JD55 (*ubr1*Δ) cells expressing either a vector control (pRS315), wild-type Ubr1 (pCH100), Ubr1^{Y277A} (pCH109), Ubr1^{Y277F} (pCH118), Ubr1^{Y277E} (pCH117), Ubr1^{K209R} (pCH157), Ubr1^{K276R} (pCH158), or Ubr1^{C1220S} (pCH159). Yeast extracts were fractionated by SDS-NuPAGE (4–12%), followed by sequential immunoblotting with antibodies to Ubr1 (Ab1$^{ScUbr1(1–1140)}$; 1:2,000) and to tubulin (1:2,000), the latter a loading/blotting control. (*E*) Pulse–chase analysis of Ubr1 proteins in JD55 (*ubr1*Δ) cells expressing either wild-type Ubr1 (pCH100), Ubr1^{Y277A} (pCH109), Ubr1^{Y277E} (pCH117), or Ubr1^{Y277F} (or pCH118). Cells were labeled for 5 min with [^{35}S]methionine/cysteine, followed by a chase for 10 and 30 min, immunoprecipitation of cell extracts with the anti-Ubr1 antibody Ab1$^{ScUbr1(1–1140)}$, SDS-6% PAGE, and autoradiography using PhosphorImager (1). (*F*) Degradation of Ubr1^{Y277E} involves pathways that involve Ubc13, Mms2 and Rad18. *S. cerevisiae* strains that carried pCH135 (which expressed flag-tagged Ubr1^{Y277E}) and were null in specific Ub-conjugating (E2) enzymes were grown to A_{600} of $\approx$1 in SC(-Leu) medium and treated with cycloheximide (50 μg/ml) for indicated times. Cell extracts were subjected to SDS-NuPAGE (4–12%) and immunoblotting with anti-flag (*Upper*) and antitubulin antibodies, the latter being a loading control. (*G*) Same as in *F*, with wild-type (BY4741), *ubc13*Δ (an experiment independent from the one in *F*) and *mms2*Δ strains. (*H*) Same as in *F*, with *rad5*Δ and *rad18*Δ strains (Table S1).

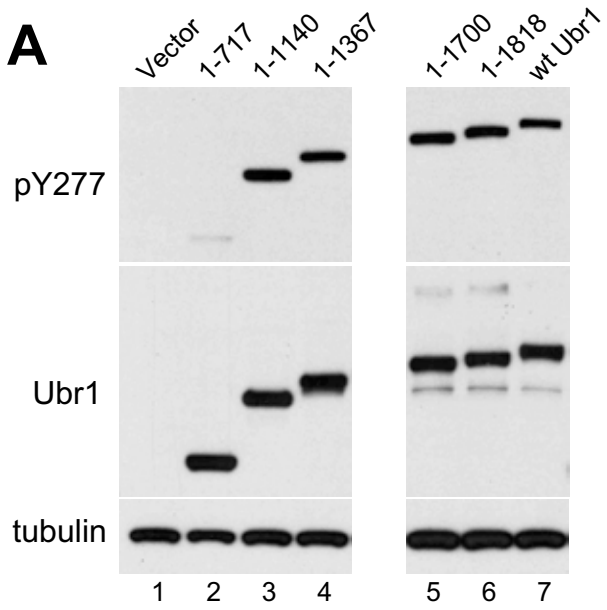

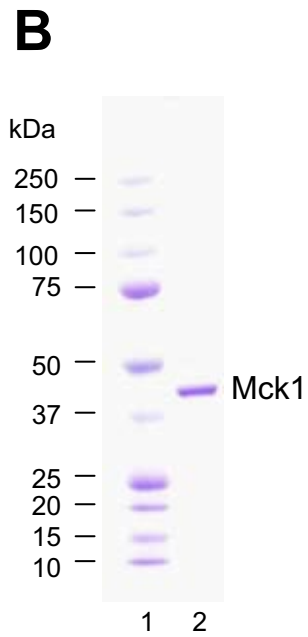

Fig. S3. C-terminal region of the 1,950-residue *S. cerevisiae* Ubr1 is required for Ubr1 phosphorylation on the N terminus-proximal Tyr^{277} residue. (*A*) Extracts from JD55 (*ubr1*Δ) cells that expressed Ubr1 or its C-terminally truncated derivatives were immunoblotted with the Ab1^{pY277Ubr1} antibody, specific for Ubr1 phosphorylated on Tyr^{277} (pY277; *Top*); with the Ab2$^{p/non\text{-}pY277Ubr1}$ antibody (*Middle*) that recognized both Ubr1^{pY277} and Ubr1 that was unphosphorylated on Tyr^{277} (see *SI Materials and Methods*), and with antitubulin antibody (*Bottom*), the latter a loading control. Lane 1, vector alone. Lane 2, Ubr1$^{1–717}$ (pNT717FlagUBR1; see Table S2). Lane 3, Ubr1$^{1–1140}$ (pUBR1NT1140Flag). Lane 4, Ubr1$^{1–1367}$ (pFlagUBR1NT1367). Lane 5, Ubr1$^{1–1700}$ (pFlagUBR1NT1700). Lane 6, Ubr1$^{1–1818}$ (pFlagUBR1NT1818). Lane 7, wild-type Ubr1 (pFlagUBR1SBX). (*B*) SDS-NuPAGE (4–12%) of purified Mck1, with staining by Coomassie. Lane 1, molecular mass markers. Lane 2, purified Mck1-ha-RGSHis$_6$ (see *SI Materials and Methods*).

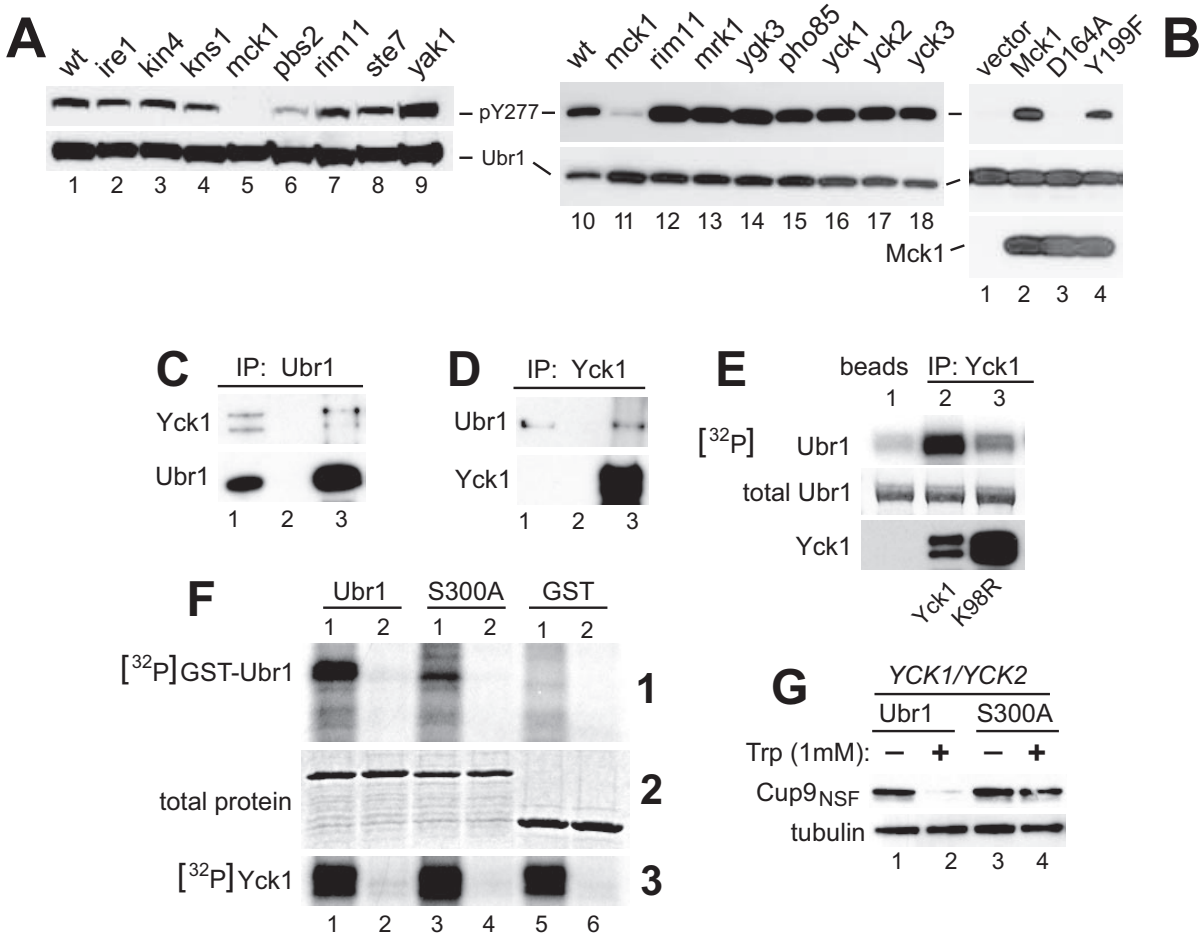

Fig. S4. (*A*) Identification of Mck1 as a cognate kinase for Ubr1 phosphorylation on Tyr^{277}. *S. cerevisiae* strains lacking specific Tyr kinases (Table S1) were transformed with ^{f}Ubr1-expressing pFlagUBR1SBX (Table S2). Cultures were grown in SC(-Leu) medium to A_{600} of ≈1, followed by SDS/PAGE of cell extracts and sequential immunoblotting with Ab1^{pY277Ubr1} and anti-flag antibodies. (*B*) BY1137 (*mck1*Δ) cells carried pFlagUBR1SBX (expressing wild-type ^{f}Ubr1) and either pRS426MET25 (vector; lane 1), or pCH206 (expressing wild-type Mck1; lane 2), or pCH207 (expressing Mck1^{D164A}; lane 3), or pCH212 (expressing Mck1^{Y199F}; lane 4). Cultures were grown to A_{600} of ≈1 in SC(-Leu,-Ura), followed by processing of extracts for SDS-NuPAGE (4–12%) and sequential immunoblotting with Ab1^{pY277Ubr1}, anti-flag, and anti-HA antibodies (the latter were used with a lower part of PVDF membrane, because of large size differences between Mck1 and Ubr1). (*C*) Coimmunoprecipitation of Ubr1 and Yck1. Lane 1, 0.25% input of extract that was used for immunoprecipitation. Extracts from JD55 (*ubr1*Δ) cells expressing ^{f}Ubr1 and Yck1-myc were incubated with beads only (lane 2) or with anti-Ubr1 (Ab1$^{ScUbr1(1–1140)}$) prebound to beads (lane 3). Bound proteins were analyzed by SDS-NuPAGE (4–12%) and immunoblotting with anti-flag and anti-myc antibodies. (*D*) Same as in *C* but extracts were incubated with beads only (lane 2) or anti-myc antibody prebound to beads (lane3) before SDS/PAGE and (parallel) immunoblotting with anti-flag and anti-myc antibodies, after cutting PVDF membrane into upper (Ubr1) and lower (Yck1) parts. Lane 1, 0.25% input of extract for immunoprecipitation. (*E*) Ubr1 is phosphorylated by Yck1. Extracts from JD55 (*ubr1*Δ) cells expressing Yck1-myc or Yck1^{K98R}-myc were incubated with beads only (lane 1) or with anti-myc antibody prebound to beads (lanes 2 and 3), followed by incubation of resuspended precipitate with γ-[^{32}]ATP, SDS-NuPAGE (4–12%), electrophoretic transfer to PVDF membrane, autoradiography (*Top*), immunoblotting with anti-myc antibody (*Bottom*), and staining with Coomassie (*Middle*; showing the band of Ubr1). (*F*) GST-Ubr1$^{227–327}$ and GST-Ubr1$^{227–327,\ S300A}$ fusion proteins were expressed in *E. coli* and purified as described in *SI Materials and Methods*. Purified GST-Ubr1$^{227–327}$, GST-Ubr1$^{227–327,\ S300A}$ or GST alone were incubated with the immunoprecipitated Yck1-myc (lane 1) or catalytically inactive Yck1^{K98R}-myc (lane 2) for 30 min at 30° C, followed by SDS/PAGE, staining of proteins by Coomassie (*Middle*) and autoradiography (*Top* and *Bottom*). *Top* and *Bottom* are ^{32}P autoradiograms in the molecular-mass regions of, respectively, GST and GST-Ubr1 fusions, and of Yck1/2. (*G*) S300A mutation in Ubr1 inhibits the Trp-induced, Ubr1-dependent acceleration of Cup9 degradation. *S. cerevisiae* CHY203 (*ubr1*Δ) carrying pRS416MET25CUP9$_{NSF}$ and either pCH100 or pCH114 (Table S2) were grown to A_{600} of ≈0.8 at 25° C in SD medium without amino acids, and thereafter incubated further in SD plus Trp (1 mM) for 30 min, followed by SDS-NuPAGE (4–12%) and immunoblotting of extracts with anti-flag (to detect Cup9$_{NSF}$) and anti-tubulin antibodies, the latter a loading/blotting control.

Table S1. *S. cerevisiae* strains used in this study

Strains	Relevant genotypes	Sources
JD52	*MATa trp1- 63 ura3–52 his3- 200 leu2–3112. lys2–801*	Ref. 1
JD55	*ubr1*::*HIS3* in JD52	Ref. 1
CHY50	*pdr5*::*KanMX6* in JD55	This study
CHY88	*mck1*::*KanMX6* in JD52	This study
CHY89	*mck1*::*KanMX6* in JD55	This study
SC295	*MATa ura3–52 leu2–3,112 regl-501 gall pep4–3*	Ref. 2
RJD347	*MATα ura3–52*	Laboratory collection
AVY26	*ubr1*::*hisG* in RJD347	Laboratory collection
LRB906	*MATa YCK1 YCK2 his3 leu2 ura3*	Ref. 3
LRB756	*MATa his3 leu2 ura3–52 yck1–1*::*ura3 yck2–2^{ts}*	Ref. 3
CHY201	*ubr1*::*KanMX6* in LRB906	This study
CHY202	*ubr1*::*KanMX6* in LRB756	This study
CHY203	*ubr1*::*SkHIS3MX6* in LRB906	This study
CHY204	*ubr1*::*SkHIS3MX6* in LRB756	This study
K601	″wild-type″ W303–1A	Ref. 4
K1305	*mck1*::*HIS3* in K601	Ref. 4
ZH35	*mck1*::*TRP1 mrk1 rim11:HIS3*	Ref. 4
ZH38	*mck1*::*TRP1 mrk1 rim11*::*HIS3 ygk3*::*LEU2* in K601	Ref. 4
ZH39	*mck1*::*TRP1 rim11*::*HIS3 ygk3*::*LEU2* in K601	Ref. 4
ZH40	*mck1*::*TRP1 mrk1 ygk3*::*LEU2* in K601	Ref. 4
ZH45	*mrk1 rim11*::*HIS3 ygk3*::*LEU2* in K601	Ref. 4
BY4741	*MATa his3–1 leu2–0 met15–0 ura3–0*	Open Biosystems
BY6589	*bub1*::*KanMX4* in BY4741	Open Biosystems
BY1428	*cka1*::*KanMX4* in BY4741	Open Biosystems
BY5693	*cmk1*:: *KanMX4* in BY4741	Open Biosystems
BY7028	*ctk1*:: *KanMX4* in BY4741	Open Biosystems
BY6774	*ctk2*:: *KanMX4* in BY4741	Open Biosystems
BY6512	*ctk3*:: *KanMX4* in BY4741	Open Biosystems
BY3798	*dun1*:: *KanMX4* in BY4741	Open Biosystems
BY4341	*gin4*:: *KanMX4* in BY4741	Open Biosystems
BY1317	*ime2*:: *KanMX4* in BY4741	Open Biosystems
BY1907	*ire1*:: *KanMX4* in BY4741	Open Biosystems
BY2489	*kin4*:: *KanMX4* in BY4741	Open Biosystems
BY1507	*kns1*:: *KanMX4* in BY4741	Open Biosystems
BY1137	*mck1*:: *KanMX4* in BY4741	Open Biosystems
BY2487	*mkk1*:: *KanMX4* in BY4741	Open Biosystems
BY2112	*mkk2*:: *KanMX4* in BY4741	Open Biosystems
BY3776	*mrk1*::*KanMX4* in BY4741	Open Biosystems
BY7101	*pbs2*:: *KanMX4* in BY4741	Open Biosystems
BY4525	*rck1*:: *KanMX4* in BY4741	Open Biosystems
BY5157	*rck2*:: *KanMX4* in BY4741	Open Biosystems
BY6745	*rim11*:: *KanMX4* in BY4741	Open Biosystems
BY802	*sky1*:: *KanMX4* in BY4741	Open Biosystems
BY3857	*ste7*:: *KanMX4* in BY4741	Open Biosystems
BY7006	*yak1*:: *KanMX4* in BY4741	Open Biosystems
BY1963	*yck1*:: *KanMX4* in BY4741	Open Biosystems
BY2058	*yck2*:: *KanMX4* in BY4741	Open Biosystems
BY6122	*yck3*:: *KanMX4* in BY4741	Open Biosystems
BY6278	*ygk3*::*KanMX4* in BY4741	Open Biosystems
BY1435	*yil042c*:: *KanMX4* in BY4741	Open Biosystems
BY5021	*ykl171w*:: *KanMX4* in BY4741	Open Biosystems
BY2797	*pho85*:: *KanMX4* in BY4741	Open Biosystems
BY4425	*ubc2*:: *KanMX4* in BY4741	Open Biosystems
BY3216	*ubc4*:: *KanMX4* in BY4741	Open Biosystems
BY3994	*ubc5*::*KanMX4* in BY4741	Open Biosystems
BY597	*ubc7*::*KanMX4* in BY4741	Open Biosystems
BY6577	*ubc8*:: *KanMX4* in BY4741	Open Biosystems
BY4763	*ubc10*:: *KanMX4* in BY4741	Open Biosystems
BY1636	*ubc11*:: *KanMX4* in BY4741	Open Biosystems
BY5214	*ubc12*:: *KanMX4* in BY4741	Open Biosystems
BY4027	*ubc13*:: *KanMX4* in BY4741	Open Biosystems
BY4454	*mms2*:: *KanMX4* in BY4741	Open Biosystems
BY3771	*bre1*:: *KanMX4* in BY4741	Open Biosystems
BY6430	*rad5*:: *KanMX4* in BY4741	Open Biosystems
BY5787	*rad18*:: *KanMX4* in BY4741	Open Biosystems

1. Ghislain M, Dohmen RJ, Levy F, Varshavsky A (1996) Cdc48p interacts with Ufd3p, a WD repeat protein required for ubiquitin-mediated proteolysis in Saccharomyces cerevisiae. *EMBO J* 15:4884–4899.
2. Du F, Navarro-Garcia F, Xia Z, Tasaki T, Varshavsky A (2002) Pairs of dipeptides synergistically activate the binding of substrate by ubiquitin ligase through dissociation of its autoinhibitory domain. *Proc Natl Acad Sci USA* 99:14110–14115.
3. Babu P, *et al*. (2002) Plasma membrane localization of the Yck2p yeast casein kinase 1 isoform requires the C-terminal extension and secretory pathway function. *J. Cell. Sci.* 115, 4957–4968.
4. Hilioti Z, *et al.* (2004) GSK-3 kinases enhance calcineurin signaling by phosphorylation of RCNs. *Genes Dev* 18:35–47.

Table S2. Plasmids used in this study

Plasmids	Descriptions	Sources
pRS315(-XbaI)UBR1	Ubr1 in pRS315	Ref.1
pFlagUBR1SBX	^{f}Ubr1 in YEplac181, with P_{ADH1} promoter and T_{CYC1} terminator	Ref. 2
pNTFlag717UBR1	$^{f}Ubr1^{1–717}$ in YEplac181, with P_{ADH1} promoter	Ref. 2
pUBR1NT1140Flag	$Ubr1^{1–1140f}$ in pFlagUBR1SBX	Ref. 2
pFlagUBRNT1367	$^{f}Ubr1^{1–1367}$ in pFlagUBR1SBX	Ref. 2
pFlagUBR1NT1700	$^{f}Ubr1^{1–1700}$ in pFlagUBR1SBX	Ref. 2
pFlagUBR1NT1818	$^{f}Ubr1^{1–1818}$ in pFlagUBR1SBX	Ref. 2
pSOB33	Ubr1 in YEp352	Ref. 3
pSS4	P_{PTR2}-LacZ in YCp50	Laboratory collection
pMET416CUP9$_{NSF}$	Cup9$_{NSF}$ in pRS416MET25	Laboratory collection
pMET416$_{F}$UPRCUP9$_{NSF}$	Flag-DHFR-Ub^{K48R}-Cup9$_{NSF}$ in pRS416MET25	Ref. 4
pRS426MET25	pRS426, with P_{MET25} promoter and T_{CYC1} terminator	Ref. 5
pGEX4T-3	N-terminal GST tag fusion plasmid	GE Healthcare
pFA6a-KanMX6	KanMX6 cassette	Ref. 6
pFA6a-SkHIS3MX6	SkHIS3 cassette	Ref. 6
pCH100	pRS315(-XbaI)UBR1 that was *SmaI*/*NotI*-cut, blunted and ligated	This study
pCH109	Ubr1^{Y277A} in pCH100	This study
pCH114	Ubr1^{S300A} in pCH100	This study
pCH117	Ubr1^{Y277E} in pCH100	This study
pCH118	Ubr1^{Y277F} in pCH100	This study
pCH119	Ubr1^{Y277F} in pFlagUBR1SBX	This study
pCH120	Ubr1^{S296A} in pFlagUBR1SBX	This study
pCH121	Ubr1^{S300A} in pFlagUBR1SBX	This study
pCH122	Ubr1^{S296A,S300A} in pFlagUBR1SBX	This study
pCH123	Ubr1$^{S292A\ ,S296A,S300A}$ in pFlagUBR1SBX	This study
pCH126	$Ubr1^{227–327}$ fragment in pGEX4T-3	This study
pCH127	$Ubr1^{227–327,Y277F}$ in pCH126	This study
pCH129	$Ubr1^{227–327,\ S300A}$ in pCH126	This study
pCH135	Ubr1^{Y277E} in pFlagUBR1SBX	This study
pCH157	Ubr1^{K209R} in pCH100	This study
pCH158	Ubr1^{K276R} in pCH100	This study
pCH159	Ubr1^{C1220S} in pCH100	This study
pCH206	Mck1-ha-RGSHis6 in pRS426MET25	This study
pCH207	Mck1^{D164A} in pCH206	This study
pCH212	Mck1^{Y199F} in pCH206	This study
pCH214	Ubr1^{T288A} in pFlagUBR1SBX	This study
pCH217	Ubr1^{S292A,S296A,S300A} in pFlagUBR1SBX	This study
pCH223	Ubr1^{S292A} in pFlagUBR1SBX	This study
pCH224	Ubr1$^{T288A,S292A,S296A,\ S300A}$ in pFlagUBR1SBX	This study
pCH246	Ubr1^{S300D} in pCH100	This study
pCH321	Yck1-myc-His_7-CC in YEplac181 with P_{ADH1} promoter T_{CYC1} terminator	This study
pCH322	Yck1^{K98R} in pCH321	This study

1. Xie Y, Varshavsky A (1999) The E2–E3 interaction in the N-end rule pathway: the RING-H2 finger of E3 is required for the synthesis of multiubiquitin chain. *EMBO J* 18:6832–6844.
2. Du F, Navarro-Garcia F, Xia Z, Tasaki T, Varshavsky A (2002) Pairs of dipeptides synergistically activate the binding of substrate by ubiquitin ligase through dissociation of its autoinhibitory domain. *Proc Natl Acad Sci USA* 99:14110–14115.
3. Bartel B, Wünning I, & Varshavsky A (1990) The recognition component of the N-end rule pathway. *EMBO J* 9:3179–3189.
4. Turner GC, Du F, Varshavsky A (2000) Peptides accelerate their uptake by activating a ubiquitin-dependent proteolytic pathway. *Nature* 405:579–583.
5. Mumberg D, Muller R, Funk M (1994) Regulatable promoters of Saccharomyces cerevisiae - comparison of transcriptional activity and their use for heterologous expression. *Nucleic Acids Res* 22:5767–5768.
6. Longtine MS, *et al.* (1998) Additional modules for versatile and economical PCR-based gene deletion and modification in *Saccharomyces cerevisiae*.*Yeast* 14:953–961.

Table S3. Some of PCR primers used in this study

Name	Sequence
OCH38	$Ubr1^{S296A}$: 5′-AAC AAC AGC AAA GAC GGC CCC CTC TAA TAG CCC TG-3′
OCH40	$Ubr1^{S96A}$: 5′-CGA GCC CCT CTA ATG CCC CTG AGG CAT CTC C-3′
OCH42	$Ubr1^{S300A}$: 5′-GCC CTG AGG CAG CTC CAT CGC TTG C-3′
OCH50	$Ubr1^{Y277A}$: 5′-GCG CAG TTT TTA AAC GAT TTA AAA GCT GAA AAC GAT TAT ATG TTT GAC GGA-3′
OCH61	Ubr1_F: 5′-AAC CCT TGT ATA GGT GTC-3′
OCH62	Ubr1_R: 5′-CTG AAA TAT TTC TCC ACC-3′
OCH63	$Ubr1^{S292A,S300A}$: 5′-CGA GCC CCT CTA ATG CCC CTG AGG CAG CT-3′
OCH65	$Ubr1^{S292A,S296A,S300A}$: 5′-AAC AAC AGC AAA GAC GGC CCC CTC TAA TGC CCC-3′
OCH75	$Ubr1^{Y277E}$: 5′-GCG CAG TTT TTA AAC GAT TTA AAA GAA GAA AAC GAT TAT ATG TTT GAC GGA AC-3′
OCH77	$Ubr1^{Y277F}$: 5′-GCG CAG TTT TTA AAC GAT TTA AAA TTT GAA AAC GAT TAT ATG TTT GAC GGA-3′
OCH278	$Ubr1^{K209R}$: 5′-TGA ATC ATT CCA TAC ATC TTC TTC TCT TAT GTC GGC ATT TGT GGC GGG ATC-3′
OCH279	$Ubr1^{K276R}$: 5′-GTC AAA CAT ATA ATC GTT TTC ATA TCT TAA ATC GTT TAA AAA CTG CGC TCT-3′
OCH327	Mck1_F: 5′-CTA GGATCC ATGTCTACGG AAGAGCAGAA TGGT-3′
OCH329	$Mck1^{D164A}$_F: 5′-GGT CTT GGC GTT TGT CAT CGT GCT ATC AAA CCA TCC AAT GTT CTT-3′
OCH330	$Mck1^{Y199F}$: 5′-CAT AAC CAG CCT TCA ATT AGT TTT ATC TGT TCA AGA TTT TAT AGA-3′
OCH338	$Ubr1^{T288A}$: 5′-GAT TAT ATG TTT GAC GGA ACA ACA GCA GCA AAG ACG AGC CCC TCT AAT AGC-3′
OCH353	$Mck1^{D164A}$_R: 5′-AAG AAC ATT GGA TGG TTT GAT AGC ACG ATG ACA AAC GCC AAG ACC-3′
OCH372	Mck1_F: 5′-AAA CTC GAG TTA GTG ATG ATG GTG ATG ATG AGA ACC TCT AGC GTA ATC TGG AAC ATC GTA TGG GTA TTC AGC AAC TTT CGT AGG TTT AAT-3′
OCH531	Yck1_F: 5′-ACA CCATG*GGT* ATGTCCATGC CCATAGCAAG TACC-3′
OCH532	Yck1_R: 5′-AAA CTC GAG TTA GTG ATG ATG GTG ATG ATG GTG *AGAACC TCT* CAG ATC TTC TTC AGA AAT AAG TTT TTG TTC ACC TAA TTT TTG GAA AAA GCC CTT-3′
OCH533	$Yck1^{K98R}$_F:3′-AAT GGC GTA CCC GTC GCG ATC AGA TTC GAG CCC AGA AAA ACG GAG-3′
OCH534	$Yck1^{K98R}$_R: 5′-CTC CGT TTT TCT GGG CTC GAA TCT GAT CGC GAC GGG TAC GCC ATT-3′

″_F″ and ″_R″ denote ″forward″ and ″reverse″ primers.